Synchronization of Homoclinic Chaos

E. Allaria, F. T. Arecchi,* A. Di Garbo,† and R. Meucci

Istituto Nazionale di Ottica Applicata, Largo E. Fermi 6, 50125 Florence, Italy

(Received 26 July 2000)

Homoclinic chaos is characterized by regular geometric orbits occurring at erratic times. Phase synchronization at the average repetition frequency is achieved by a tiny periodic modulation of a control parameter. An experiment has been carried on a CO_2 laser with feedback, set in a parameter range where homoclinic chaos occurs. Any offset of the modulation frequency from the average induces phase slips over long times. Perfect phase synchronization is recovered by slow changes of the modulation frequency based upon the sign and amplitude of the slip rate. Satellite synchronization regimes are also realized, with variable numbers of homoclinic spikes per period of the modulation.

Homoclinic chaos of the Shilnikov type, initially observed in chemical [1] and laser [2] experiments, shows striking similarities with the electrical spike trains traveling on the axons of animal neurons [3]. More generally, chemical oscillators based on an activator-inhibitor competition, which rule biological clocks controlling living rhythms, such as the heart pacemaker, hormone production, metabolism, etc., display rhythmical trains of spikes with erratic repetition frequency as shown in Refs. [1,2]. These rhythms cannot be reduced to two dimensional dynamics, as instead it is the case of artificial clocks which are based on stable limit cycles [4–7].

The geometry of homoclinic chaos consists of regular orbits in phase space, which repeat themselves with a very small spatial variance. This regularity makes it difficult to extract relevant chaotic indicators from the geometry of the measured time series. Time wise however, the return period of these orbits is widely fluctuating, with very weak correlation between two successive returns [8,9]. Being the most apparent feature, it is convenient to characterize homoclinic chaos through the statistics of the return intervals [10,11]. The return map of successive return intervals consists of many branches which cross the fixed point line at a steep angle, so that successive iterations are sparse over the plane rather than clustered along the diagonal, as it should be for correlated sequences. Such a lack of correlation appears as a pseudo-Markovian behavior, even though it is purely deterministic. However the highly unstable character of the return map makes the homoclinic chaos extremely vulnerable to noise [12], ruling out the hope of a practical way of controlling it.

On the other hand, the main concern in the dynamics of biological rhythms is to exploit the synchronization mechanisms, such as those which occur in large neuron assemblies during perceptual tasks, called "feature binding" [13,14] or those associated with an external periodic driving, such as the circadian rhythms [4–6]. Chaotic synchronization has been introduced as the identical behavior of two coupled chaotic systems [15], later extended to the case of only phase correlation of the two systems [16], or as the phase locking of a single chaotic system with respect to an external forcing [17]. In this latter respect, extensive theoretical investigations of Rössler [18] and Lorenz models [19,20] have been provided. On the experimental side, chaotic synchronization has been exploited for communication with lasers [21] and its relevance demonstrated in some physiological phenomena (heartbeat [22], electrosensitive neurons [23]); however, quantitative assessments on sensitivity and operational range of the synchronization phenomenon have not been provided so far.

In this Letter we report a viable method of homoclinic synchronization, showing its robustness notwithstanding the above mentioned fast decorrelation. We provide experimental evidence of such a synchronization on a laser operating in a homoclinic chaos regime [2], to which we add a small periodic modulation of a control parameter. When the modulation frequency is close to the "natural frequency," that is, to the average frequency of the return intervals, the required modulation is below 1%. An increased modulation amplitude up to 2% provides a wide synchronization domain which attracts a frequency range of 30% around the natural frequency. However, as we move away from the natural frequency, the synchronization is imperfect insofar as phase slips, that is, phase jumps of $\pm 2\pi$, appear. We show how to eliminate these phase slips by a long time control of the modulation frequency, based upon the sign and amplitude of the slip rate.

Furthermore, applying a large negative detuning with respect to the natural frequency gives rise to synchronized bursts of homoclinic spikes separated by approximately the average period, but occurring in groups of 2, 3, etc. within the same modulation period (locking 1:2, 1:3, etc.) and with a wide intergroup separation. A similar phenomenon occurs for large positive detunings; this time the spikes repeat regularly every 2, 3, etc. periods (locking 2:1, 3:1, etc.). Also these locking regimes are affected by phase slips, which can be eliminated by the same procedure presented here for the 1:1 case.

A dynamical model, which will be presented elsewhere, reproduces with quantitative accuracy all the relevant

features above reported and provides a sound basis for a heuristic interpretation of these phenomena as well as a motivation for their widespread occurrence.

The experiment has been performed on a single mode CO_2 laser with a feedback proportional to the output intensity. Precisely, a photon detector converts the laser output intensity into a voltage signal, which is fed back through an amplifier to an intracavity electro-optic modulator, in order to control the amount of cavity losses. The average voltage on the modulator and the ripple around it are controlled by adjusting the bias and gain of the amplifier. We set these two control parameters so that the laser intensity displays a large spike above zero, followed by a fast damped train of a few oscillations and a successive longer train of chaotic bursts which on average appear as a growing oscillation (Fig. 1). Damped and growing trains represent, respectively, the approach to, and the escape from, an unstable equilibrium point from where the trajectory rapidly returns to zero and then starts a new orbit. The average orbital period is around 500 μs. A suitable characterization of this regime can be provided by the return time of the main spike to a threshold level. A digital oscilloscope records the laser output with a sampling time of 5 μs. From this time series we collect the times $(t_j: j = 1, 2, \ldots, M)$ at which the laser intensity crosses, with positive derivative, a threshold centered at 70% of the main peak. By using the set $\{t_j\}$ we define the average return interval as $T = \frac{1}{M-1} \sum_{j=1}^{j=M-1} (t_{j+1} - t_j)$. This value has been used to select an appropriate frequency range for the applied forcing. As for the control parameter to be modulated, we can choose either the bias voltage of the feedback ampli-
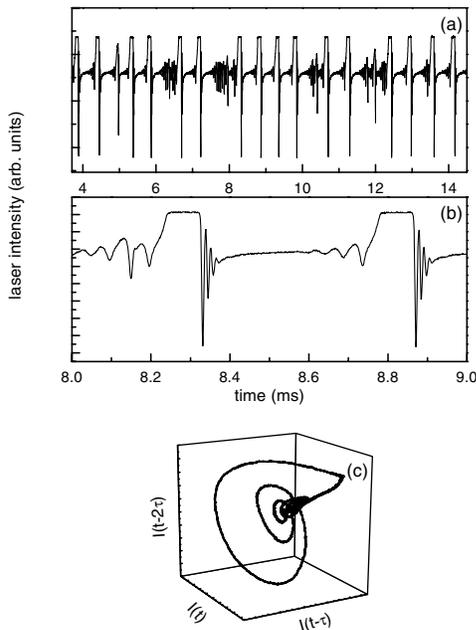
fier or the pump of the gain medium. As our phenomena are relatively slow (around 2 kHz) we can safely modulate the discharge current of the laser tube, thus modifying the pump parameter from P_0 to $P_0[1 + m \sin(2\pi ft)]$. The values of m and f explored in the experiment are reported in Fig. 3.

For a given modulation period T_{mod}, the phase locking states are characterized by evaluating the quantity $R = \frac{T}{T_{mod}}$ for different values of the modulation amplitude. The existence of a (p:q) phase locking state obviously implies that $R = \frac{p}{q}$. Different phase locking regimes have been reported in Fig. 2 together with the applied sinusoidal forcing. The main phase synchronization domain (1:1) is reported in Fig. 3a as a function of the amplitude V and frequency ν of the applied forcing. The criterion used to assign a point to the domain is that the R values be maintained for almost ten periods. The behavior of R as a function of the forcing frequency is reported in Fig. 3b for two values of the modulation amplitude.

It is worth noticing that the adopted criterion to define the phase locking domain does not guarantee perfect phase synchronization for all times. To provide a better

FIG. 1. (a) Experimental time series of the laser intensity for a CO_2 laser with feedback, in the regime of homoclinic chaos. (b) Time expansion of a single orbit. (c) Trajectory built by an embedding technique with appropriate delays.
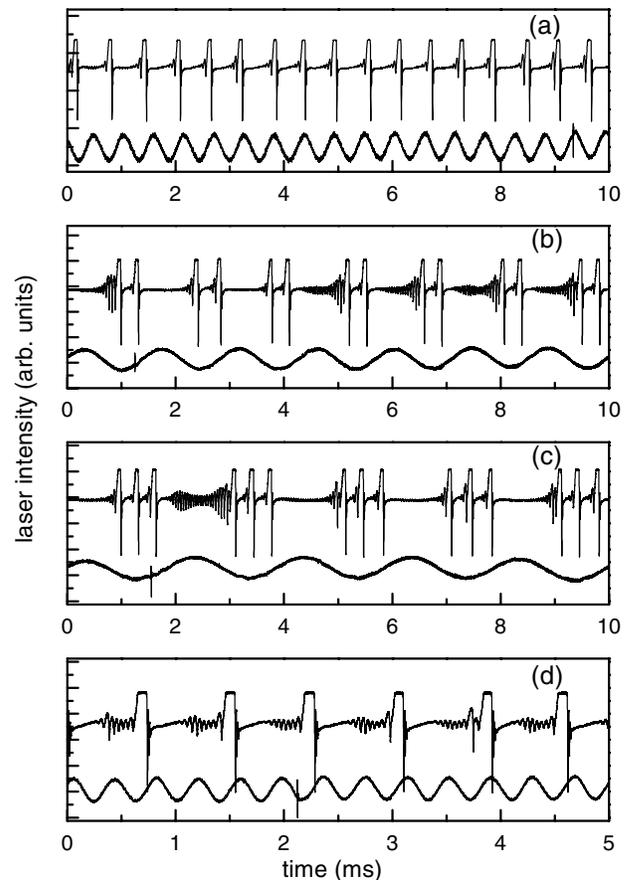

FIG. 2. Experimental time series for different phase synchronizations induced by a frequency modulated control parameter. For comparison time plots of the modulation control parameter are reported for each case. The modulation frequencies are, respectively, (a) 1:1 at 1.6 kHz; (b) 1:2 at 0.7 kHz; (c) 1:3 at 0.5 kHz; (d) 2:1 at 2.6 kHz.
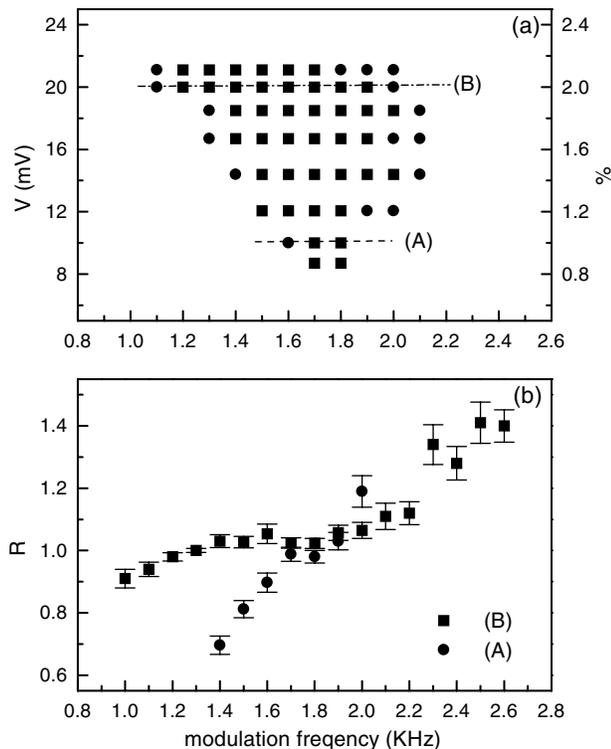
FIG. 3. (a) Phase synchronization domain for the 1:1 locking ratio. Vertical axis: modulation amplitude in mV and %; horizontal axis: modulation frequency in kHz. The domain edge points (black circles) correspond to a phase slip more frequent than any ten returns. (b) Locking parameter R versus the modulation frequency for the two amplitudes 10 mV (circles) and 20 mV (squares).

FIG. 4. (a) Phase slips at different frequencies for the 20 mV amplitude (horizontal line B in Fig. 3a). The dynamical system monotonically lags or leads in phase depending on whether the modulation frequency is above or below the perfect synchronization (no slips) value of 1.6 kHz. (b) Expanded view of the time in a phase slip. The phase slip is like a defect in a periodic one-dimensional pattern; in fact in this case it is a missed return to the surface of section.

understanding of phase synchronization in our system we explore the possible occurrence of phase slips. By this we mean that at certain times the phase difference between the laser output and the modulation signal shows jumps of integer multiples of 2π. The phase of the laser intensity is defined as $\varphi(t) = 2\pi n(t)$, where $n(t)$ is the number of spikes occurring in a time interval t. In Fig. 4 we report the phase difference between the laser output intensity and the modulation $S(t) = \varphi(t) - 2\pi\nu t$ for different $\nu's$ within the synchronization domain corresponding to 1:1 locking. Departing from the perfect synchronization (zero phase slip) and approaching the edges of the domain the slip rate increases. This phenomenon of imperfect phase synchronization has been studied theoretically in the forced Lorenz system [19,20].

Here we exploit the slip rate information to readjust the value of the modulation frequency in order to reach perfect synchronization. Precisely, we introduce the average phase slip rate $(dS/dt)_{\Delta t}$ defined as the number of jumps S divided by the number Δt of periods of the modulation over which the former number has been evaluated, $(dS/dt)_{\Delta t}$ goes to zero at the natural frequency (Fig. 4a); otherwise there is a lead or a lag depending on whether the modulation frequency is below or above the natural frequency, respectively. Furthermore, the chaotic character of the slip occurrences is shown by the variance
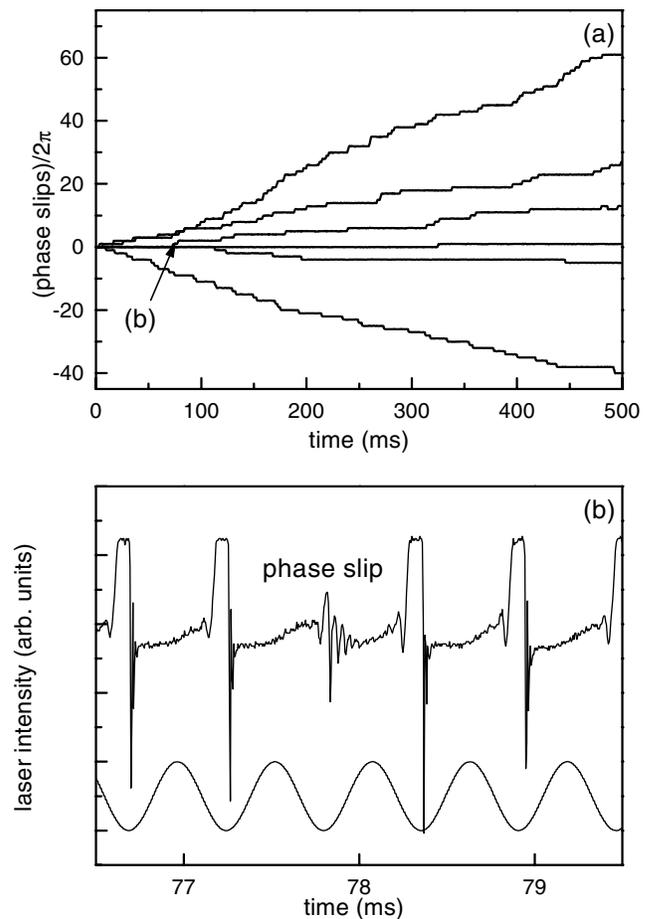
$\langle[(dS/dt)_{\Delta t} - \langle(dS/dt)\rangle]^2\rangle$, where the angular brackets denote an average over very large Δt. The control consists in applying increments $\Delta\nu = -a(dS/dt)_{\Delta t}$ ($a > 0$ being a suitable coefficient) to the modulation frequency at every time increment Δt, so that the modulation frequency as a function of time is given by $\nu(t) = \nu_0 + \sum \Delta\nu(t)$, where ν_0 is the unperturbed modulation frequency, and the sum being extended over all the intervals Δt up to time t.

In the experiment, we compare the output signal with the modulation signal over a time interval Δt, evaluate the slip rate $(dS/dt)_{\Delta t}$, and readjust correspondingly the frequency of a waveform generator which modulates the laser power supply. If Δt is small, local fluctuations from the average yield a bad control, whereas for large Δt the slip rate has a small variance, thus we expect an asymptotic Δt beyond which the slip rate becomes negligible, as confirmed by the experiment (Fig. 5). Of course, the persistent application of such a control brings the modified modulation frequency asymptotically close to the natural frequency.
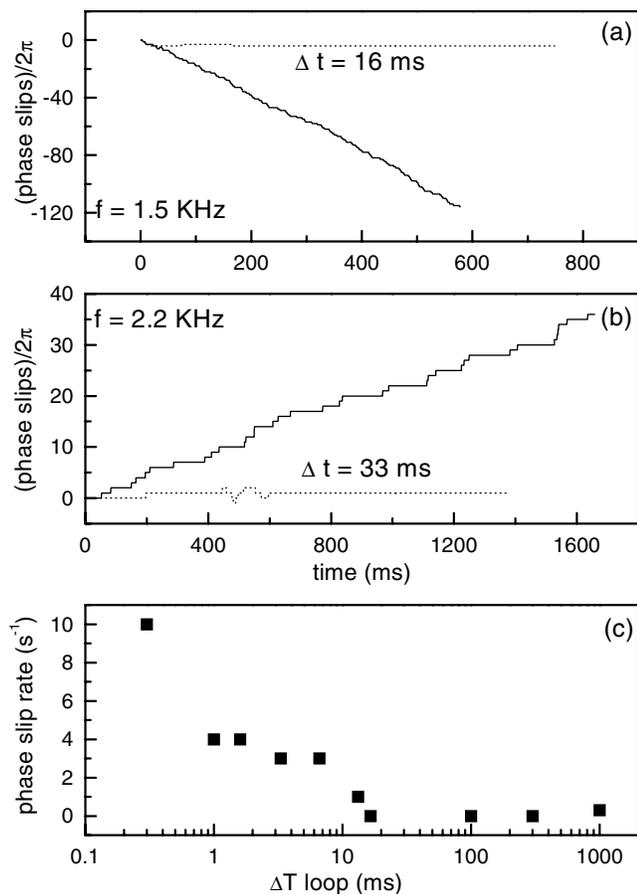
FIG. 5. Long time correction of the phase slip in two cases where the uncontrolled frequency setting of the modulation is below (a) or above (b) the frequency corresponding to the perfect synchronization; solid and dotted lines represent the uncontrolled and controlled cases, respectively. (c) Dependence of the residual phase slip upon the sampling time in the case (b).

In conclusion, we have shown that homoclinic chaos can be synchronized by use of the temporal information contained in the main spikes. This type of chaos however cannot be controlled due to the decorrelation of the successive return times; this feature is due to the frequent leaps among the many unstable periodic orbits contained within the chaotic attractor. The synchronization is perfect as the modulation frequency matches the average return frequency. As we move away from this condition, we measure an increasing amount of phase slip. This however can be controlled by a secondary feedback loop which acts on the modulation frequency, that is, which controls the control parameter. Since the secondary loop acts on the time scale of the phase slip, it represents a long time perturbation as compared to the modulation. Thus, our dynamical system resembles the combination of short-term memory and long-term memory hypothesized in some dynamical models of the brain behavior [24].

*Also with the Departement of Physics, University of Firenze, Italy.
†Also with the Istituto di Biofisica CNR, Via Alfieri 1, Ghezzano Pisa, Italy.

[1] F. Argoul, A. Arnéodo, and P. Richetti, J. Chem. Phys. **84**, 1367 (1987).
[2] F. T. Arecchi, R. Meucci, and W. Gadomski, Phys. Rev. Lett. **58**, 2205 (1987).
[3] A. L. Hodgkin and A. F. Huxley, J. Physiol. (London) **117**, 500 (1952).
[4] A. T. Winfree, *The Geometry of Biological Time* (Springer-Verlag, New York, 1980).
[5] A. Goldbeter, *Biochemical Oscillations and Cellular Rhythms* (Cambridge University Press, Cambridge, 1996).
[6] J. Keener and J. Sneyd, *Mathematical Physiology* (Springer-Verlag, New York, 1998).
[7] See three Focus Issues of Chaos; **1**, n. 3 (1991) (Nonlinear dynamics of physiological control); **5**, n. 1–4 (1995) (Dynamical disease: mathematical analysis of human illness); **6**, n. 3 (1996) (Synchronization and patterns in complex systems).
[8] L. P. Sil'nikov, Sov. Math. Dokl. **6**, 163 (1965).
[9] A. Arneodo, P. Coullet, E. A. Spiegel, and C. Tresser, Physica (Amsterdam) **14D**, 327 (1985).
[10] F. T. Arecchi, A. Lapucci, R. Meucci, G. A. Roversi, and P. H. Coullet, Europhys. Lett. **6**, 677 (1988).
[11] F. T. Arecchi, W. Gadomski, A. Lapucci, H. Mancini, R. Meucci, and G. A. Roversi, J. Opt. Soc. Am. B **5**, 1153 (1988).
[12] F. T. Arecchi, A. Lapucci, and R. Meucci, Physica (Amsterdam) **62D**, 186 (1993).
[13] C. von der Malsburg and W. Schneider, Biol. Cybernet. **54**, 29 (1986).
[14] W. Singer, Concepts Neuroscience **1**, 1 (1990).
[15] L. M. Pecora and T. L. Carroll, Phys. Rev. Lett. **64**, 821 (1990).
[16] M. G. Rosenblum, A. S. Pikovsky, and J. Kurths, Phys. Rev. Lett. **76**, 1804 (1996).
[17] A. S. Pikovsky, M. G. Rosenblum, G. V. Osipov, and J. Kurths, Physica (Amsterdam) **104D**, 219 (1997).
[18] A. S. Pikovsky, M. A. Zaks, M. G. Rosenblum, G. V. Osipov, and J. Kurths, Chaos **7**, 680 (1997).
[19] M. A. Zaks, E. H. Park, M. G. Rosenblum, and J. Kurths, Phys. Rev. Lett. **82**, 4228 (1999).
[20] E. H. Park, M. A. Zaks, and J. Kurths, Phys. Rev. E **60**, 6627 (1999).
[21] G. D. VanWiggeren and R. Roy, Science **279**, 1198 (1998).
[22] C. Schafer, M. G. Rosenblum, J. Kurths, and H. H. Abel, Nature (London) **392**, 239 (1998).
[23] A. Neiman, X. Pei, D. Russell, W. Wojtenek, L. Wilkens, F. Moss, H. A. Braun, M. T. Huber, and K. Voigt, Phys. Rev. Let. **82**, 660 (1999).
[24] S. Grossberg, Neural Netw. **1**, 17 (1988).